

2D Anisotropic Photonic Crystals of Hollow Semiconductor Nanorod with Liquid Crystals

Filiz Karaomerlioglu^{1,a}, Sevket Simsek^{2,b}, Amirullah M. Mamedov^{2,c},
Ekmel Ozbay^{2,d}

¹Department of Electronic and Computer Education, Mersin University, Mersin, Turkey

²Nanotechnology Research Center (NANOTAM), Bilkent University 06800, Ankara, Turkey

^afilizkrm@mersin.edu.tr, ^bsevkets@bilkent.edu.tr, ^cmamedov@bilkent.edu.tr, ^dozbay@bilkent.edu.tr

Keywords: Anisotropic Photonic Crystal, Semiconductor, Liquid Crystal

Abstract. Photonic crystals (PCs) have many applications in order to control light-wave propagation. A novel type of two-dimensional anisotropic PC is investigated band gap and optical properties as a hollow semiconductor nanorod with nematicliquid crystals (LC). The PC structure composed of an anisotropic nematicLC in semiconductor square hollow nanorod is designed using the plane wave expansion (PWE) method and finite-difference time-domain (FDTD) method. It has been used 5CB (4-pentyl-4'-cyanobiphenyl) as LC core, and Tellurium (Te) as square hollow nanorod material. The PC with hollow Tenanorod with nematicLC is compared with the PC with solid Tenanorod and the PC with hollow Tenanorod.

Introduction

Progress in solid-state physics, optics of spatially structures, and nanotechnologies based on a variety of the physical and chemical processes has strongly stimulated and motivated the investigation into the properties of photonic crystals and resulted in the growth of applications of photonic band-gap materials, i.e. artificially structured materials where optical parameters are periodically modulated in space with a period of a unit photonic crystal cell on the order of the optical wavelength. Previous studies about photonic band-gap structures (PBG), photonic band-gap materials, and photonic crystals (PCs) are important investigations [1,2]. The basic feature of PCs is the presence of permitted and forbidden frequency bands for light. It is possible to manipulate the light with PCs. Due to this property, PCs hold a great potential for designing new optical devices. There has been an increase in researches of tuning the optical properties of photonic band gap to design devices. Some tunable photonic band gap researches have been done in one-dimensional (1D) [3] and two dimensional (2D) [4-11] and 3D [12] PCs.

Materials are very important to determine the optical properties of a PC. The properties of PCs made of anisotropic materials different from those of isotropic PCs. Zabel and Stroud have been reported that the anisotropy of materials can split degenerate bands and this will close band gap of the PC [13]. Li et al. have proved that the band gap can be increased by using the anisotropic materials in a PC [14]. B. Rezaei and M. Kalafianalyzed the tunability of full band gap of anisotropic tellurium rods infiltrated with LCs in air background [15] and 2D hexagonal PC of circular rods consisting of an inner rod and anisotropic outer shell aligned in a uniform background [16]. B. Rezaei et al. are studied the absolute band gap properties of 2D PCs created by square, triangular and honeycomb lattices of air holes in anisotropic tellurium background by changing the shape and orientation of the holes [17]. Liu showed that the absolute bandgaps can be continuously tuned in the square and triangular lattices consisting of anisotropic-dielectric cylinders by infiltrating nematicLC [18]. Liu et al. are theoretically demonstrated the tunable bandgaps in 3D anisotropic PC structure with nematic LCs [19]. Pan et al. calculated absolute photonic band gaps for oval hollow anisotropic tellurium (Te) rods and square hollow anisotropic Te rods for the triangular and the square lattice [20].

In present paper, we theoretically demonstrated and developed the band gaps and optical properties in 2D anisotropic PC structure with nematic LCs. PC structure and materials were especially selected that optical properties are changed by external effect such as an electric field, magnetic field, light, temperature etc. The investigation is achieved by controlling intensity of band gap and optical properties added different material to a certain structure. The band gap is manipulated by rotating directors of LCs under the impact of an applied electric field. It was solved Maxwell's equations for the propagation of electromagnetic waves in a periodic arrangement of anisotropic PC with nematic LCs. Using the PWE method and FDTD method, the PC structure composed of an anisotropic LC in semiconductor square hollow nanorod is designed.

Numerical Method

The fundamentals of the PWE method and the FDTD method are based on a direct numerical solution of the time-dependent Maxwell's equations as illustrated in some articles [21-26]. Generally LCs possess two kinds of dielectric constants. One is ordinary dielectric constants ϵ_o , and the other is extraordinary dielectric constants ϵ_e . Light waves with electric fields perpendicular and parallel to the director of the LC have ordinary and extraordinary refractive indices, respectively. The components of the dielectric tensor of the nematic LC are represented as [27]

$$\begin{aligned} \epsilon_{xx}(\vec{r}) &= n_o^2 + (n_e^2 - n_o^2) \cos^2 \theta \cos^2 \phi & (1) \\ \epsilon_{xy}(\vec{r}) &= \epsilon_{yx}(\vec{r}) = (n_e^2 - n_o^2) \cos^2 \theta \sin \phi \cos \phi & (2) \\ \epsilon_{xz}(\vec{r}) &= \epsilon_{zx}(\vec{r}) = (n_e^2 - n_o^2) \sin \theta \cos \theta \cos \phi & (3) \\ \epsilon_{yy}(\vec{r}) &= n_o^2 + (n_e^2 - n_o^2) \cos^2 \theta \sin^2 \phi & (4) \\ \epsilon_{yz}(\vec{r}) &= \epsilon_{zy}(\vec{r}) = (n_e^2 - n_o^2) \sin \theta \cos \theta \sin \phi & (5) \\ \epsilon_{zz}(\vec{r}) &= n_o^2 + (n_e^2 - n_o^2) \sin^2 \theta & (6) \end{aligned}$$

where θ is the tilt angle of the LC director (i.e. the angle between the LC director and the XY-plane) and ϕ is the rotation angle between the projection of the LC director on the XY-plane and the X-axis, and \vec{n} is the director of the LC.

On the other hand Bloch's theorem [28] is used to expand the $H(\vec{r})$ field in terms of plane waves since the light waves are transmitted in periodic structures, as

$$H(\vec{r}) = \sum_{\vec{G}} h(\vec{G}) \hat{e}_{\vec{G}} e^{i(\vec{k} + \vec{G}) \cdot \vec{r}} \tag{7}$$

where \vec{k} is a wave vector in the Brillouin zone of the lattice and $\hat{e}_{\vec{G}}$ is the direction which is perpendicular to the wave vector $(\vec{k} + \vec{G})$ owing to the transverse character of the magnetic field $H(\vec{r})$, $\nabla \cdot H(\vec{r}) = 0$.

2D Anisotropic PCs with LCs

A novel type of two-dimensional anisotropic PC structure composed of an anisotropic nematic LC in semiconductor square hollow nanorod with lattice constant $a = 1 \mu m$ is presented. The PC structures are depicted in Fig. 1. It has considered (a) anisotropic Tenanorod, (b) hollow anisotropic Tenanorod, and (c) hollow anisotropic Tenanorod of nematic LC-infilled in air background ($\epsilon_a = 1$) for square lattice. Anisotropic Tenanorod has two different principle refractive indices as ordinary refractive index $n_o = 4.8$ and extraordinary refractive index $n_e = 6.2$. The ordinary and extraordinary refractive index of 5CB type (4-pentyl-4'-cyanobiphenyl) LCs are $n_o = 1.548$ and $n_e = 1.742$, respectively. Parameters d_1 and d_2 denote the inner and outer length of anisotropic Tenanorods, respectively.

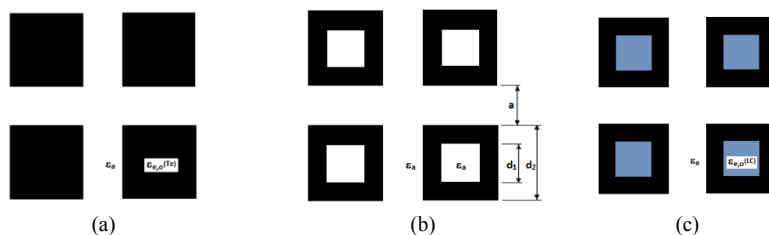


Fig. 1. For square lattice (a) anisotropic Tenanorod, (b) hollow anisotropic Tenanorod, and (c) hollow anisotropic Tenanorod of nematic LC-infiltrated in air background.

Firstly, it is considered photonic band structure for square lattice of anisotropic solid Tenanorod in air background. It is assumed that $d_2 = 0.6a$, the sides of square nanorod parallel to the primitive reciprocal lattice vectors. The PBG map for TE and TM mode which is calculated along to the high symmetry point for Brillouin zone in square lattice is plotted in Fig. 2. Relative width and center normalized frequency values are seen that two band gaps for TE modes and three band gaps for TM modes as shown in Table 1. Solving for TE band polarization it is founded TE1 band gap value from band 1 to band 2, TE2 value from band 3 to band 4. Similarly, TM1 gap size is 19.6 % between band 1 and band 2, TM2 is 13.3% between band 3 and band 4, and TM3 is 8.5% between band 6 and band 7 for TM band polarization.

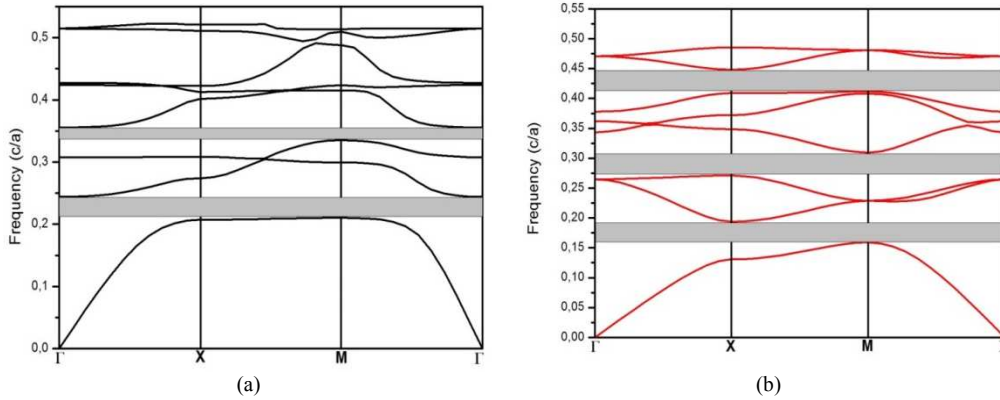


Fig. 2. Photonic band gap for (a) TE and (b) TM mode in square lattice of anisotropic Tenanorod in air background.

Table 1. Photonic band gap and gap size % of TE and TM modes for square lattice of anisotropic Tenanorod in air background

TM		TE	
BandGap [$\omega a/2\pi c$]	Gap Size %	BandGap [$\omega a/2\pi c$]	Gap Size %
TM1 (0.159-0.193)	19.6	TE1 (0.210-0.244)	14.8
TM2 (0.271-0.309)	13.3	TE2 (0.335-0.356)	5.9
TM3 (0.411-0.448)	8.5		

Secondly, photonic band structure of hollow anisotropic Tenanorod in air background is considered. It is assumed that $d_1 = 0.3a$ and $d_2 = 0.6a$ denote the inner and outer length of hollow anisotropic Tenanorods. The band diagram for the second pattern is plotted in Fig. 3. When anisotropic Tenanorod is compared with hollow anisotropic Tenanorod, it is seen that variation of band gap number for TE mode is decreased and for TM mode is increased. Table 2 shows relative width and center normalized frequency values of hollow anisotropic Tenanorod in air background.

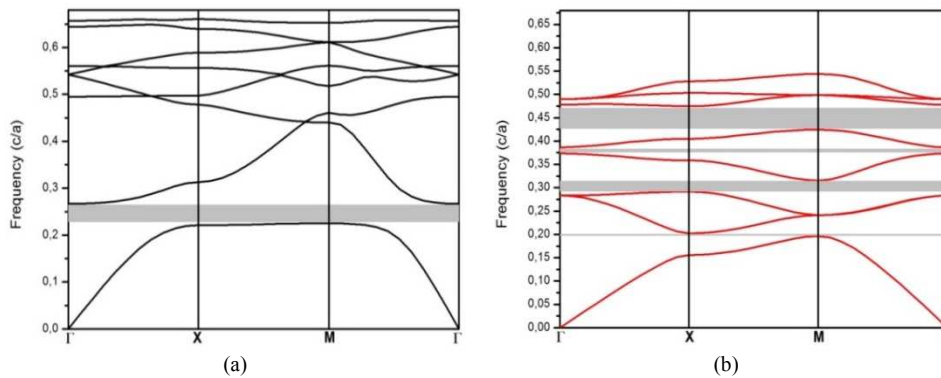


Fig. 3. Photonic band gap for (a) TE and (b) TM mode in square lattice of hollow anisotropic Tenanorod in air background.

Table 2. Photonic band gap and gap size % of TE and TM modes for square lattice of hollow anisotropic Tenanorod in air background

TM			TE		
	BandGap[$\omega a/2\pi c$]	Gap Size %	BandGap [$\omega a/2\pi c$]	Gap Size %	
TM1	(0.196-0.202)	2.9	TE1	(0.225-0.267)	16.9
TM2	(0.291-0.315)	7.9			
TM3	(0.373-0.386)	3.5			
TM4	(0.424-0.474)	11.2			

Fig. 4 indicates the photonic band structure of hollow anisotropic Tenanorod of nematic LC-infiltrated in air background for square lattice. For TE and TM modes band gap size of hollow anisotropic Tenanorod of nematic LC- infiltrated approximately is closed of hollow anisotropic Tenanorod as shown in Table 3. Compared hollow anisotropic Tenanorod of nematic LC-infiltrated in air background with hollow anisotropic Tenanorod in air background, it can be seen that band gap number increase in TE mode, and band gap number is the same in TM mode but band gap values are changed.

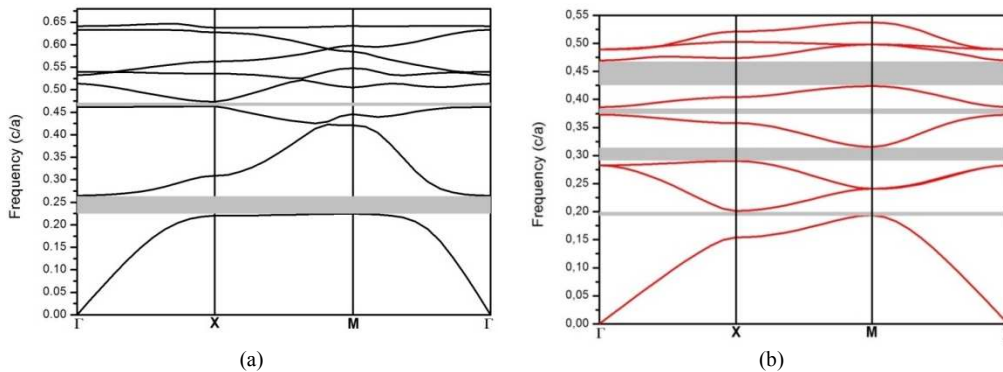


Fig. 4. Photonic band gap for (a) TE and (b) TM mode in square lattice of hollow anisotropic Tenanorod of nematic LC-infiltrated in air background.

Table 3. Photonic band gap and gap size % of TE and TM modes for square lattice of hollow anisotropic Tenanorod of nematic LC-infiltrated in air background

TM			TE		
	BandGap[$\omega a/2\pi c$]	Gap Size %	BandGap [$\omega a/2\pi c$]	Gap Size %	
TM1	(0.193-0.201)	4.0	TE1	(0.224-0.265)	16.8
TM2	(0.290-0.315)	8.2	TE2	(0.463-0.473)	2.2
TM3	(0.372-0.386)	3.5			
TM4	(0.423-0.469)	10.2			

It is well known that anisotropic nanostructuring PBG structure array are capable of changing the polarization state of transmitted or reflected light. Therefore we also calculated optical response of PBG structure for different rotation angle of the polarization ellipse and ellipticity of light transmitted through PBG array. The numerical results of variation of full band gap by changing the director of LC for photonic crystal structure rotated fully from 0° to 90° presents in Tables 4-5 and Fig. 5. Variation of band gap size % as a function of θ is demonstrated for TE mode and TM mode in square lattice of hollow anisotropic Tenanorod of nematic LC-infiltrated in air background show that TE mode is not affected excessively from rotated photonic crystal structure (Fig. 5 (a)). The most widely gap affecting TE band structures are between 30° and 60°. Particularly, while TE5 band gap is reached maximum value, TE2, TE4 and TE6 band gaps are closed at $\theta = 45^\circ$. On the other hand, Fig. 5 (b) is indicated that TM band structures are more delicate to rotate angle of photonic crystal struc-

ture. The most important point at $\theta = 45^\circ$ unlike TE band gaps, TM band gaps reach to the minimum value. Furthermore, TM1 band gap which has the lowest frequency in TM mode are not altered via rotate angle.

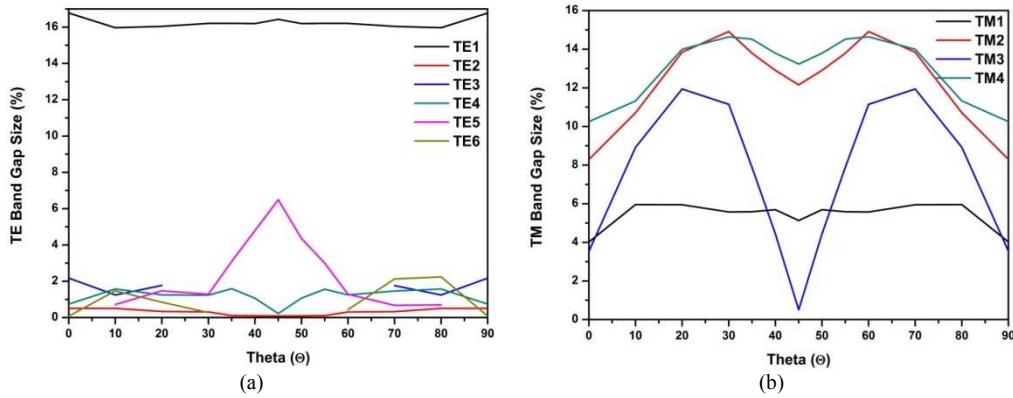


Fig. 5. Variation of bandgap size as a function of θ for (a) TE and (b) TM mode in square lattice of hollow anisotropic Tenanorod of nematic LC-infiltrated in air background.

Table 4. Variation of full band gap size for TE modes in square lattice of LC-infiltrated anisotropic tellurium nanorodin air background.

θ^0	TE1		TE2		TE3		TE4		TE5		TE6	
	BandGap [$\omega a/2\pi c$]	Gap Size %	BandGap [$\omega a/2\pi c$]	Gap Size %	BandGap [$\omega a/2\pi c$]	Gap Size %	BandGap [$\omega a/2\pi c$]	Gap Size %	BandGap [$\omega a/2\pi c$]	Gap Size %	BandGap [$\omega a/2\pi c$]	Gap Size %
0	(0.224-0.265)	16.77	(0.423-0.425)	0.52	(0.463-0.473)	2.17	(0.522-0.525)	0.75	(0.590-0.591)	0.07	(0.634-0.638)	0.72
10	(0.231-0.271)	15.97	(0.438-0.440)	0.51	(0.481-0.487)	1.25	(0.535-0.543)	1.58	(0.567-0.571)	0.72	(0.602-0.611)	1.47
20	(0.231-0.271)	16.04	(0.444-0.446)	0.33	(0.487-0.496)	1.77	(0.538-0.545)	1.25	(0.567-0.576)	1.47	(0.614-0.619)	0.85
30	(0.229-0.270)	16.21	(0.449-0.451)	0.31	-	-	(0.534-0.540)	1.23	(0.567-0.574)	1.28	(0.621-0.623)	0.28
35	(0.230-0.271)	16.21	(0.454-0.455)	0.10	-	-	(0.536-0.545)	1.59	(0.569-0.586)	3.08	-	-
40	(0.230-0.271)	16.17	(0.454-0.455)	0.09	-	-	(0.537-0.542)	1.07	(0.565-0.593)	4.79	-	-
45	(0.225-0.266)	16.42	(0.445-0.446)	0.09	-	-	(0.525-0.527)	0.22	(0.549-0.586)	6.49	-	-
50	(0.230-0.271)	16.17	(0.454-0.455)	0.09	-	-	(0.537-0.542)	1.07	(0.565-0.591)	4.36	-	-
55	(0.230-0.271)	16.21	(0.454-0.455)	0.10	-	-	(0.536-0.545)	1.59	(0.569-0.586)	3.08	-	-
60	(0.229-0.270)	16.21	(0.449-0.451)	0.31	-	-	(0.534-0.540)	1.23	(0.567-0.574)	1.28	(0.621-0.624)	0.44
70	(0.231-0.271)	16.04	(0.444-0.446)	0.33	(0.487-0.496)	1.77	(0.537-0.545)	1.46	(0.569-0.572)	0.68	(0.612-0.625)	2.13
80	(0.231-0.271)	15.97	(0.438-0.440)	0.51	(0.481-0.487)	1.25	(0.535-0.543)	1.58	(0.567-0.571)	0.72	(0.602-0.616)	2.24
90	(0.224-0.265)	16.77	(0.423-0.425)	0.52	(0.463-0.473)	2.17	(0.522-0.525)	0.75	(0.590-0.591)	0.07	(0.634-0.638)	0.72

Table 5. Variation of full band gap size for TM modes in square lattice of LC-infiltrated anisotropic tellurium nanorodin air background.

θ^0	TM1		TM2		TM3		TM4	
	BandGap [$\omega a/2\pi c$]	Gap Size %	BandGap [$\omega a/2\pi c$]	Gap Size %	BandGap [$\omega a/2\pi c$]	Gap Size %	BandGap [$\omega a/2\pi c$]	Gap Size %
0	(0.193-0.201)	4.02	(0.290-0.315)	8.29	(0.372-0.386)	3.54	(0.423-0.469)	10.25
10	(0.195-0.207)	5.95	(0.295-0.328)	10.71	(0.370-0.405)	8.92	(0.431-0.483)	11.32
20	(0.196-0.208)	5.94	(0.297-0.341)	13.84	(0.367-0.414)	11.94	(0.425-0.489)	13.99
30	(0.197-0.209)	5.58	(0.297-0.345)	14.91	(0.368-0.411)	11.14	(0.423-0.490)	14.64
35	(0.197-0.209)	5.58	(0.298-0.343)	13.79	(0.374-0.405)	7.88	(0.424-0.490)	14.52

40	(0.197-0.208)	5.69	(0.299-0.340)	12.90	(0.381-0.398)	4.43	(0.426-0.489)	13.79
45	(0.195-0.205)	5.13	(0.295-0.334)	12.15	(0.384-0.386)	0.51	(0.421-0.480)	13.23
50	(0.197-0.208)	5.69	(0.299-0.340)	12.90	(0.381-0.398)	4.43	(0.426-0.489)	13.79
55	(0.198-0.208)	5.58	(0.298-0.343)	13.79	(0.374-0.405)	7.88	(0.424-0.490)	14.52
60	(0.197-0.209)	5.58	(0.297-0.208)	14.91	(0.368-0.411)	11.14	(0.423-0.490)	14.64
70	(0.196-0.208)	5.94	(0.297-0.341)	13.84	(0.367-0.414)	11.94	(0.425-0.489)	13.99
80	(0.195-0.207)	5.95	(0.295-0.328)	10.71	(0.370-0.405)	8.92	(0.431-0.483)	11.32
90	(0.193-0.201)	4.02	(0.290-0.315)	8.29	(0.372-0.386)	3.54	(0.423-0.469)	10.25

Fig. 6 is shown as variation of TE bandgap size and TM bandgap size as a function of n_e and n_o for square lattice of hollow anisotropic Tenanorod of nematic LC-infiltrated in air background. As seen in Fig. 6 (a) there exist two photonic band gaps in TE band structure. It is clear that TE1 band gap size is more sensitive than TE2 band gap size to anisotropic refractive index. TE2 band gap quite is low for $n_e < 4$ and $n_o < 2$. Moreover, the variation of n_e is more influenced TE1 band gap than n_o . On the other hand, TE1 band gap is close to zero for $n_e \leq 4$ and $n_o \leq 4$. It can be seen from Fig. 6 (b) that TM band structure of square lattice of hollow anisotropic Tenanorod of nematic LC-infiltrated have fully four band gaps (TM1, TM2, TM3 and TM4). The variation of this band gaps according to anisotropic refractive index are similar to each other. In contrast TE band gap size, it is seen in Fig. 6 (b) that TM band gap size is linearly depended on anisotropic refractive index.

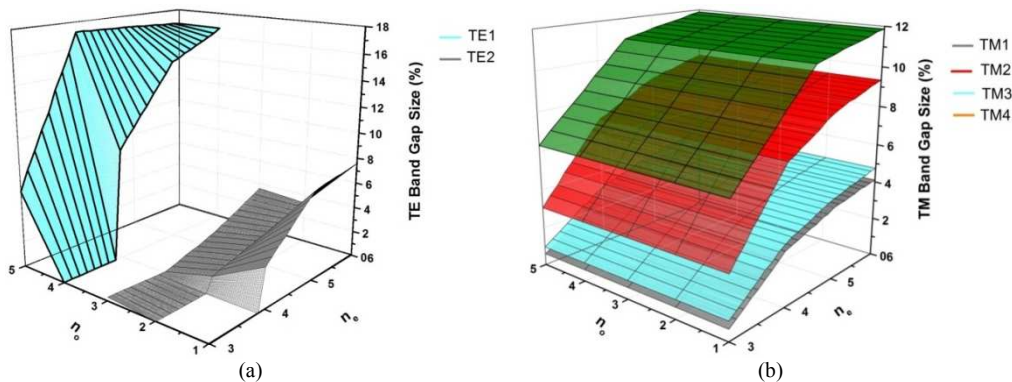


Fig. 6. Variation of TE band gap size and TM band gap size as a function of n_e and n_o for square lattice of hollow anisotropic Tenanorod of nematic LC-infiltrated in air background.

Conclusion

It was theoretically studied the optical properties in 2D anisotropic PC structure modulated by nematic LCs. The investigation was achieved by selecting convenient structure and materials. The PC structure consisted of an anisotropic nematic LC (5CB) in semiconductor (Te) square hollow nanorod is designed using the PWE method and the FDTD method. Numerical results were shown that optical properties of the photonic structure can be controlled by rotating directors of LC. When photonic crystal structure rotated fully from 0° to 90° , absolute band gap existed between 40° and 50° .

References

- [1] E. Yablonovitch, J. Opt. Soc. Am. B Vol. 10 (1993), p. 283.
- [2] J.N. Winn, R.D. Meade, J.D. Joannopoulos, J. Mod. Optics Vol. 41 (1994), p. 257.
- [3] G. Alagappan, X. W. Sun, P. Shum, M. B. Yu, M. T. Doan, J. Opt. Soc. Am. B Vol. 23 (2006), p. 159.
- [4] C.S. Kee, H. Lim, Phys. Rev. B Vol. 64 (2001), p. 121103-1.
- [5] S.M. Hsu, M.M. Chen, H.C. Chang, Opt. Express Vol. 15 (2007), p. 5416.
- [6] C. Schuller, F. Klopff, J.P. Reithmaier, M. Kamp, A. Forchel, Appl. Phys. Lett. Vol. 82 (2003), p. 2767.

- [7] D. Liu, Y. Gao, D. Gao, X. Han, *Optics Commun.* Vol. 285 (2012), p. 1988.
- [8] N. Zhu, J. Wang, C. Cheng, X. Yan, *Optik* Vol. 124 (2013), p. 309.
- [9] Z.Y. Li, B.Y. Gu, G.Z. Yang, *Phy. Rev. Lett.* Vol. 81 (1998), p. 2574.
- [10] H. Takeda, K. Yoshino, *Phy. Lett. E* Vol. 70 (2004), p. 026601-1.
- [11] G. Alagappan, X. W. Sun, P. Shum, M. B. Yu, D. den Engelsen, *J. Opt. Soc. Am. A* Vol. 23 (2006), p. 2002.
- [12] K. M. Ho, C. T. Chan, C. M. Soukoulis, *Phys. Rev. Lett.* Vol. 65 (1990), p. 3152.
- [13] I. H. H. Zabel, D. Stroud, *Phys. Rev. B* Vol. 48 (1993), p. 5004.
- [14] Z. Y. Li, J. Wang, B.Y. Gu, *Phys. Rev. B* Vol. 58 (1998), p. 3721.
- [15] B. Rezaei, M. Kalafi, *Optics Commun.* Vol. 282 (2009), p. 1584.
- [16] B. Rezaei, M. Kalafi, *Optics Commun.* Vol. 266 (2006), p. 159.
- [17] B. Rezaei, T. F. Khalkhali, A. S. Vala, M. Kalafi, *Optics Commun.* Vol. 282 (2009), p. 2861.
- [18] C.-Y. Liu, *Phy. Lett. A* Vol. 372 (2008), p. 5198.
- [19] C.-Y. Liu, Y.-T. Peng, J.-Z. Wang, L.-W. Chen, *Physica B* Vol. 388 (2007), p. 124.
- [20] T. Pan, F. Zhuang, Z. Y. Li, *Solid State Commun.* Vol. 129 (2004), p. 501.
- [21] C.Y. Liu, L.W. Chen, *IEEE Photonics Techn. Lett.* Vol. 16 (2004), p. 1849.
- [22] C.Y. Liu, L.W. Chen, *J. of Nanomaterials* Vol. 2006 (2006), p. 1.
- [23] A. Taflove, in: *Advances in Computational Electrodynamics: The Finite-Difference Time-Domain Method*, chapter, 1, Artech House, Boston, Mass, USA, (1998).
- [24] Z. Ma, K. Ogusu, , *Optics Commun.* Vol. 282 (2009), p. 1322.
- [25] M. Plihal, A. A. Maradudin, *Phys. Rev. B* Vol. 44 (1991), p. 8565.
- [26] J.D. Joannopoulos, R.D. Meade, J.N. Winn, in: *Photonic Crystals: Molding the Flow of Light*, chapter, 2, second ed., Princeton University Press, Princeton, NJ, (1995).
- [27] I.-C. Khoo, S.-T. Wu, in: *Optics and Nonlinear Optics of Liquid Crystals*, chapter, 2, World Scientific, Singapore, (1993).
- [28] Kittel, Charles, in: *Introduction to Solid State Physics*, chapter, 7, Wiley, New York, (1996).

Mechatronics, Applied Mechanics and Energy Engineering

10.4028/www.scientific.net/AMM.394

2D Anisotropic Photonic Crystals of Hollow Semiconductor Nanorod with Liquid Crystals

10.4028/www.scientific.net/AMM.394.38